

ABSTRACT

This paper proposes a performance modular multilevel converter for DC-DC converter for photo voltaic applications. This converter will provide a constant voltage of 48 volts for a resistive load. The best suitable point for operation of this converter and settling time is calculated through simulation in this paper.

INTRODUCTION

Due to increase in demand of electrical power supply in human life, it is necessary to meet the demand. On the other hand due to exhaust of conventional resources the main focus of power developing industries is opting for renewable energy resources. The most commonly is solar energy. The photo voltaic energy systems will takes the input sun radiation and produces DC output. Fig.1 shows the basic diagram of photovoltaic array connected to grid through Dc-Dc converter.

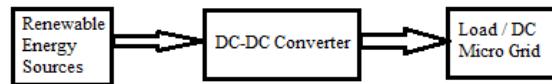


Fig.1 Block diagram of DC based PV array

Several industries are opting for multi level converters to reduce switching losses and switching stress.

PROPOSED CONVERTER CONFIGURATION

In this paper, the flying capacitor and full-bridge converters are combined to get modular multilevel Dc-Dc converters for the high step-down and high power dc-based conversion applications. Due to the charging and discharging balance of the built-in flying capacitor, the input voltage auto-balance ability is naturally realized, which halves the switch voltage stress and overcomes the input voltage imbalance. The concept of modular multilevel dc/dc converters may provide a clear picture on high-voltage Dc-Dc topologies for the dc-based distribution and microgrid systems. The propose converter configuration is shown in below Fig.2.

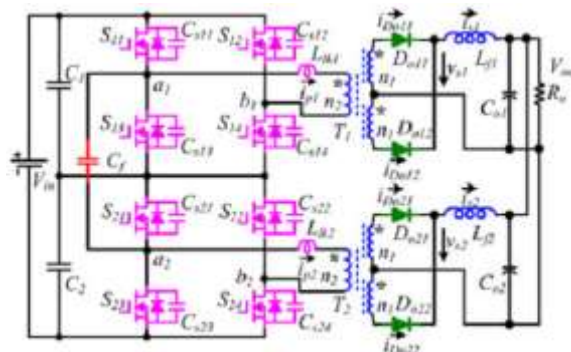


Fig.2 Proposed converter configuration

OPERATION OF PROPOSED CONVERTER

This converter operation is divided in to eight parts. The model wave forms representing the operation are shown in Fig.3.

Mode.1 [t₀-t₁]: Before t₁, the switches S₁₁,S₁₄,S₂₁, andS₂₄are in the turn-on state to deliver the power to the secondary side. The output diodes D_{o11} and D_{o21} are conducted and the output diodes D_{o12} and D_{o22} are reverse biased. The flying capacitor C_f is in parallel with the input divided capacitor C1 to make V_{Cf} equal toV_{C1}. The primary currents i_{p1} and i_{p2} are expressed as follows, which is increased to the peak value at the end of this mode as shown in Fig.4 (a).

$$i_{p1}(t) = i_{p1}(t_0) + \frac{V_{in}/2 - NV_{out}}{L_{lk1} + N^2 L_{f1}}(t - t_0)$$

$$i_{p2}(t) = i_{p2}(t_0) + \frac{V_{in}/2 - NV_{out}}{L_{lk2} + N^2 L_{f2}}(t - t_0).$$

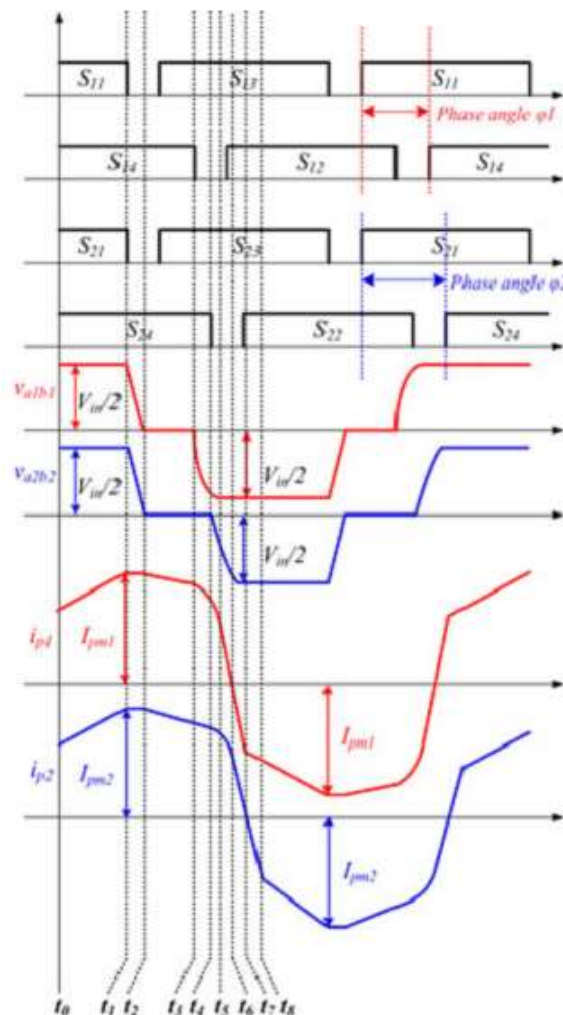


Fig.3 Waveforms of proposed converter

Mode.2 [t₁-t₂]: At t₁, the turn-off signals of the switches S₁₁ and S₂₁ are given. ZVS turn off for these two switches are achieved due to the capacitors C_{s11} and C_{s21}. C_{s11} and C_{s21} are charged and C_{s13} and C_{s23} are discharged by the primary currents.

Mode.3 [t₂-t₃]: At t₂, the voltages of C_{s13} and C_{s23} reach zero and the body diodes of S₁₃ and S₂₃ are conducted, providing the ZVS turn-on condition for S₁₃ and S₂₃. The flying capacitor C_f is changed to be in parallel with the input divided capacitor C₂. The primary currents are given as

$$i_{p1}(t) = \frac{i_{s1}(t)}{N}$$

$$i_{p2}(t) = \frac{i_{s2}(t)}{N}.$$

Mode.4 [t₃-t₄]: At t₃, S₁₄ turns off with ZVS. C_{s14} is charged and C_{s12} is discharged, leading to the forward bias of D_{o12} hence, the secondary current circulates freely through both D_{o11} and D_{o12}. i_{p1} is regulated by

$$i_{p1}(t) = i_{p1}(t_3) \cos \omega(t - t_3)$$

Mode.5 [t₄-t₅]: At t₄, the turn-off signal of S₂₄ comes. ZVS turn-off performance is achieved for S₂₄. Similar to the previous time interval, D_{o21} and D_{o22} conduct simultaneously, thus leading to the transformer T₂ short-circuit. i_{p2} is regulated by

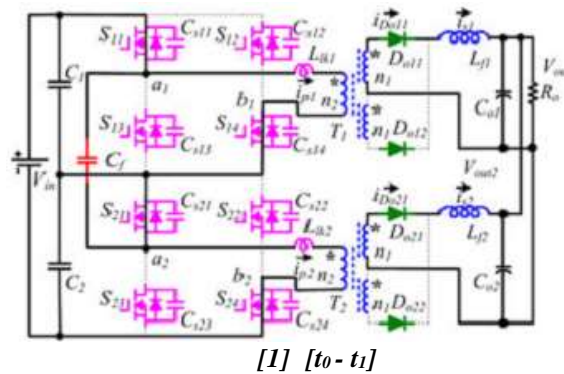
Mode.6 [t₅-t₆]: At t₅, C_{s12} is discharged completely and the anti parallel diode of S₁₂ conducts, getting ready for the ZVS Turn-on of S₁₂. During this time interval, i_{p1} declines steeply due to half-input voltage across the leakage inductor L_{lk1}. i_{p1} is given by

$$i_{p1}(t) = i_{p1}(t_5) - \frac{V_{in}/2}{L_{lk1}}(t - t_5).$$

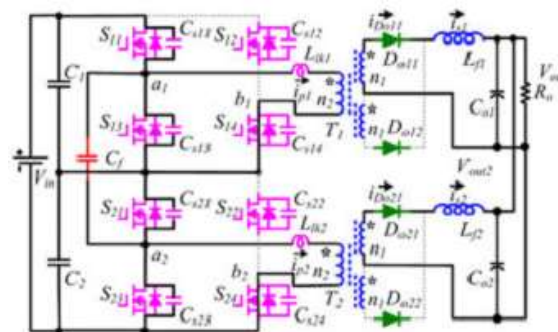
Mode.7 [t₆-t₇]: At t₆, i_{p1} decreases to 0 and increases reversely with the same slope through S₁₂ and S₁₃. C_{s22} is discharged completely and the anti-parallel diode of S₂₂ conducts. i_{p2} declines rapidly due to half-input voltage across the leakage inductor L_{lk2}. i_{p2} is given by

$$i_{p2}(t) = i_{p2}(t_6) - \frac{V_{in}/2}{L_{lk2}}(t - t_6).$$

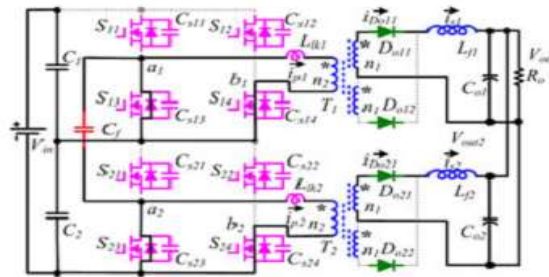
Mode.8 [t₇-t₈]: At t₇, i_{p2} decreases to 0 and increases reversely through S₂₂ and S₂₃. The current through the output diode D_{o11} decreases to 0 and turns off. The output diode D_{o21} turns off after t₈, and then a similar operation works in the remaining stages.



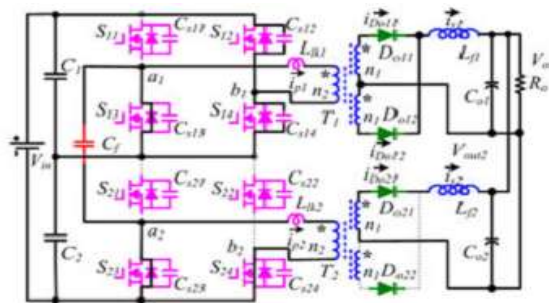
[1] [t₀ - t₁]



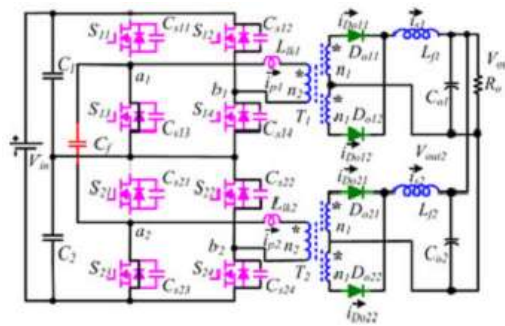
[2] [t₁ - t₂]



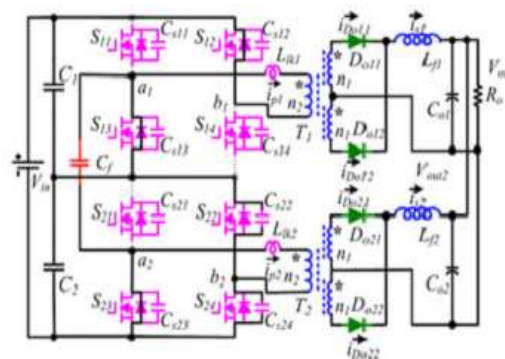
[3] $[t_2 - t_3]$



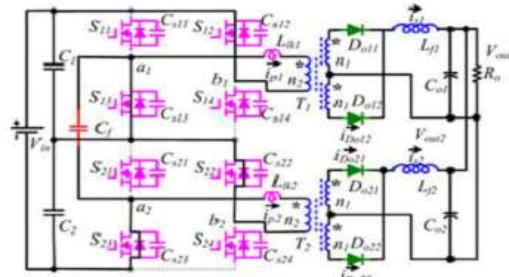
[4] $[t_3 - t_4]$



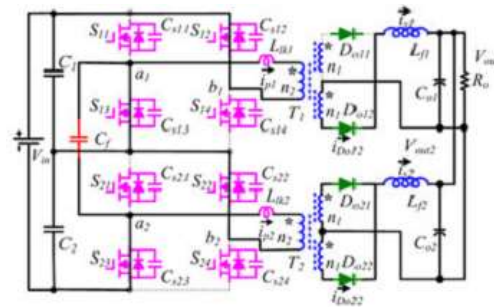
[5] $[t_4 - t_5]$



[6] $[t_5 - t_6]$



[7] [t6 - t7]



[8] [t7 - t8]

Fig.4 Modes of operation of proposed converter

SIMULATION & RESULTS

A PV array having 1662 series connected cells will develop a voltage of 600V. This PV array voltage is shown in

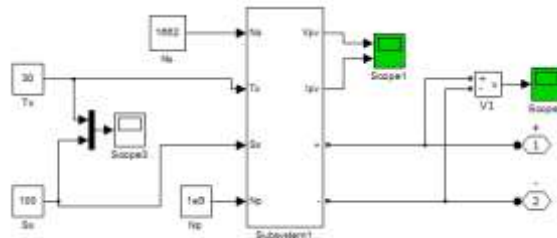


Fig.5 Simulink implementation of solar cell

Simulink implementation of proposed converter is shown in Fig.6. This converter is controlled by switching pulses shown in Fig.7. The voltage across flying capacitor is half of the applied voltage 300V. It is shown in Fig.9. The output voltage of 48V is shown in Fig 10.

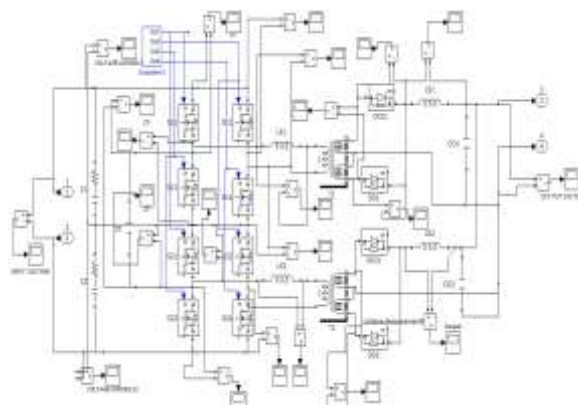


Fig.6 Modular Multi-level Dc-Dc Converter

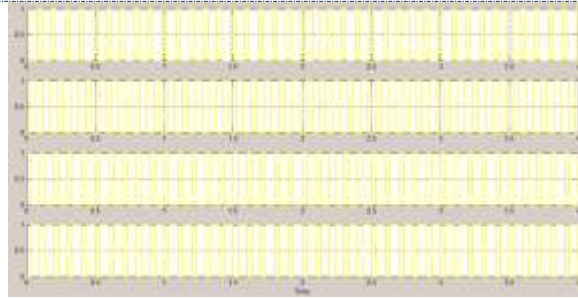


Fig.7 Switching Pulses

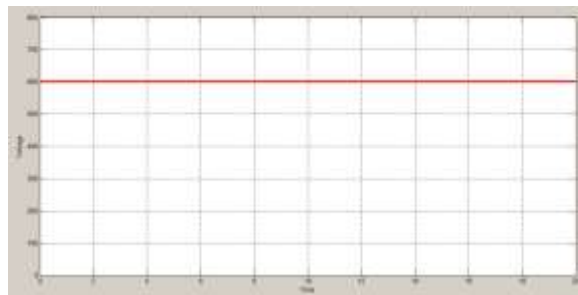


Fig.8 PV panel array voltage



Fig.9 Voltage across flying capacitor

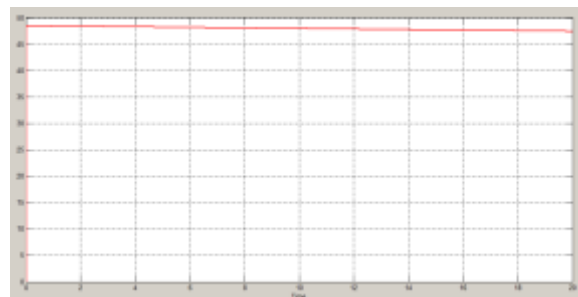


Fig. 10 Output voltage waveform

The performance of this converter is analyzed by applying different values of loads are shown in Fig.11.

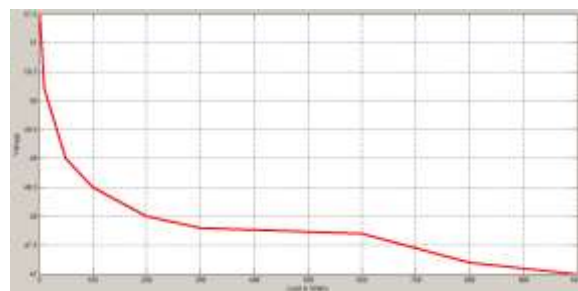


Fig.11 Variation of load voltage

CONCLUSION

The proposed converter gives an output voltage of 48V at 400W load. This configuration will provides ripple free voltage which is advantageous for microgrid operations.

REFERENCES

1. H. Kakigano, Y. Miura, and T. Ise, "Low-voltage bipolar-type DC microgrid for super high quality distribution," *IEEE Trans. Power Electron.*, vol. 25, no. 12, pp. 3066–3075, Dec. 2010.
2. S. Anand and B. G. Fernandes, "Reduced-order model and stability analysis of low-voltage DC microgrid," *IEEE Trans. Ind. Electron.*, vol. 60, no. 11, pp. 5040–5049, Nov. 2013.
3. S. Anand and B. G. Fernandes, "Optimal voltage level for DC microgrids," in *Proc. IEEE Conf. Ind. Electron.*, 2010, pp. 3034–3039.
4. D. Salomonsson, L. Soder, and A. Sannino, "An adaptive control system for a DC microgrid for data centers," *IEEE Trans. Ind. Appl.*, vol. 44, no. 6, pp. 1910–1917, Nov./Dec. 2008.
5. K. B. Park, G. W. Moon, and M. J. Youn, "Series-input series-rectifier interleaved forward converter with a common transformer reset circuit for high-input-voltage applications," *IEEE Trans. Power Electron.*, vol. 26, no. 11, pp. 3242–3253, Nov. 2011.
6. T. Qain and B. Lehman, "Coupled input-series and output-parallel dual interleaved flyback converter for high input voltage application," *IEEE Trans. Power Electron.*, vol. 23, no. 1, pp. 88–95, Jan. 2008.
7. C. H. Chien, Y. H. Wang, B. R. Lin, and C. H. Liu, "Implementation of an interleaved resonant converter for high-voltage applications," *Proc. IET Power Electron.*, vol. 5, no. 4, pp. 447–455, Apr. 2012.
8. C. H. Chien, Y. H. Wang, and B. R. Lin, "Analysis of a novel resonant converter with series connected transformers," *Proc. IET Power Electron.*, vol. 6, no. 3, pp. 611–623, Mar. 2013.
9. W. Li, Y. He, X. He, Y. Sun, F. Wang, and L. Ma, "Series asymmetrical half-bridge converters with voltage autobalance for high input-voltage applications," *IEEE Trans. Power Electron.*, vol. 28, no. 8, pp. 3665–3674, Aug. 2013.
10. T. T. Sun, H. S. H. Chung, and A. Ioinovici, "A high-voltage DC-DC converter with $V_{in}/3$ —Voltage stress on the primary switches," *IEEE Trans. Power Electron.*, vol. 22, no. 6, pp. 2124–2137, Nov. 2007.
11. T. T. Sun, H. Wang, H. S. H. Chung, S. Tapuhi, and A. Ioinovici, "A highvoltage ZVZCS DC-DC converter with low voltage stress," *IEEE Trans. Power Electron.*, vol. 23, no. 6, pp. 2630–2647, Nov. 2008.
12. H. Wang, H. S. H. Chung, and A. Ioinovici, "A class of high-input lowoutput voltage single-step converters with low voltage stress on the primary-side switches and high output current capacity," *IEEE Trans. Power Electron.*, vol. 26, no. 6, pp. 1659–1672, Jun. 2011.
13. J. R. Pinheiro and I. Barbi, "The three-level ZVS PWM converter—A new concept in high voltage DC-to-DC conversion," in *Proc. IEEE Int. Conf. Ind. Electron. Control Instrum. Autom.*, 1992, pp. 173–178.
14. R. Xinbo, L. Zhou, and Y. Yan, "Soft-switching PWM three-level converters," *IEEE Trans. Power Electron.*, vol. 16, no. 5, pp. 612–622, Sep. 2001.
15. W. Li, S. Zong, F. Liu, H. Yang, X. He, and B. Wu, "Secondary-side phase-shift-controlled ZVS DC/DC converter with wide voltage gain for high input voltage applications," *IEEE Trans. Power Electron.*, vol. 28, no. 11, pp. 5128–5139, Nov. 2013.
16. J. S. Lai and F. Z. Peng, "Multilevel converters—A new breed of power converters," *IEEE Trans. Ind. Appl.*, vol. 32, no. 3, pp. 509–517, May/Jun.1996.
17. R. Giri, V. Choudhary, R. Ayyanar, and N. Mohan, "Common-duty-ratiocontrol of input-series connected modular DC-DC converters with active input voltage and load-current sharing," *IEEE Trans. Ind. Appl.*, vol. 42, no. 4, pp. 1101–1111, Jul./Aug. 2006.
18. J. Shi, J. Luo, and X. He, "Common-duty-ratio control of input-series output-parallel connected phase-shift full-bridge DC-DC converter modules," *IEEE Trans. Power Electron.*, vol. 26, no. 11, pp. 3318–3329, Nov.2011.